3D printing of continuous flax fibre reinforced biocomposites for structural applications

A. Le Duigou, A. Barbé, E. Guillou, M. Castro

3D PRINTING OF CONTINUOUS FLAX FIBRE REINFORCED BIOCOMPOSITES FOR STRUCTURAL APPLICATIONS

A. Le Duigou[1*], A. Barbé[2], E. Guillou[1] and M. Castro[1]

[1] IRDL UMR CNRS 6027, Université de Bretagne Sud, Lorient France
[2] Compositic, Université de Bretagne Sud, Lorient France

*Corresponding author: antoine.le-duigou@univ-ubs.fr

Tel: +33297874586 / Fax: +33297874588

Abstract

Recently, interest has been increasing in natural fibres as composite reinforcing fillers for polymer-based filaments manufactured with the Fused Deposition Modeling (FDM) process, despite their moderate mechanical properties compared to pure polymer.

An innovative way was proposed in the present work to optimize the mechanical properties of biocomposites. It was based on novel continuous flax fibre/PLA (cFF/PLA) composite filaments made with a customized co-extrusion process and printed with a simple and affordable printing machine. The microstructure of the printed cFF/PLA biocomposite evidenced a homogeneous distribution of yarn within the cross section, while the twisted flax yarn led to fibre-rich areas at mesoscale. The cFF/PLA showed tensile modulus and strength values that exceeded the only available published result on continuous natural fibre printed composites by more than 4.5 times. Tensile properties were in the same range as those for continuous glass fibre/PolyAmide (PA) printed composites, paving the way for the use of biocomposites in structural applications. Their weakest point was their transverse properties that remained poorer than similar flax/PLA thermocompressed composites.

Keywords: 3D printing, natural fibres, mechanical properties

1. Introduction

Among several AM techniques, Fused Deposition Modeling (FDM - also known as Fused Filament Fabrication (FFF)) can be performed on thermoplastic polymers or composites, to allow a filament to be printed in layers. The main benefits of FDM are its low cost, relatively high speed and potential for reinventing the design process [1]. Nevertheless today several drawbacks remain, such as the limited availability of materials, the numerous printing parameters (layer thickness, width, orientation) and their moderate mechanical performance which hinder their more extensive development, especially for load bearing applications [2].

Thermoplastic polymers reinforced with natural fibres (wood, flax, hemp, etc.) possess a promising range of specific mechanical properties [3] in combination with a reduced environmental footprint [4]. These biocomposites are most commonly used in manufacturing process such as extrusion, injection moulding, thermoforming, film stacking, vacuum bag moulding, etc. [3][5][6]. Recently, natural fibres have been attracting interest as composite fillers for 3D printing, but the mechanical properties of the printed parts remain low. This can be explained by the poor properties of selected fibres, the low volume fraction, the low fibre aspect ratio, the fibre disorientation, and the high porosity content in the printed part [7][8][9][10].

Continuous synthetic (glass, carbon or aramid) fibre composites are increasingly being studied due to the high level of performance they can achieve compared to their discontinuous counterparts [11]. 3D Printing can be performed with simultaneous impregnation of polymer and fibres [12][13][14] or on pre-impregnated filaments [15][16][17], the latter exhibiting higher potential for structural applications with significantly improved mechanical performance.

As far as we know, Matsuzaki *et al.* [13] were the first authors to propose the printing of continuous natural fibres (jute yarn) with a PLA matrix using a simultaneous impregnation process. The obtained mechanical performance exceed all the published data available for 3D printed discontinuous natural fibre composites, with a longitudinal stiffness of 5.11 ± 0.41 GPa, strength of 57.1 ± 5.3 MPa and strain at failure of 1.81 ± 0.44%. However, jute fibres properties are moderate compared to other natural fibres [18], the fibre content was low (vf = 6.1%) while the linear density of jute yarn was high (500 Tex) [13].

Based on the above, the purpose of this study was to evaluate the mechanical performance of a novel high-performance 3D printed biocomposite based on a continuous flax yarn embedded in a PLA matrix. Flax fibres were selected because of their tensile properties, which are among the best available in the natural fibre range [19]. In addition, flax yarns are industrially available with a very high quality and a large range of linear density. Continuous flax/PLA biocomposite filaments (cFF/PLA) were produced here using a customized co-extrusion process. The microstructure of the filament was studied including porosity, dispersion and fibre content. Then, a simple and affordable 3D printer was modified to enable the printing of the developed cFF/PLA filaments. The microstructure of the final 3D printed part was then characterized by image analysis, while tensile mechanical properties were evaluated in the longitudinal and transverse directions. Finally, performance was analyzed in terms of material microstructure and compared with the literature.

2. Material and methods

2.1 Materials

Continuous flax yarns were provided by SAFILIN. The selected yarn was twisted (320 Turn/meter) with a linear density of 68 Tex. Polylactic acid Ingeo^{TM} Biopolymer 3260HP

(PLA) provided by NatureWorks® was used with the following rheological properties: MFR=65 g/10min at 210°C.

2.2 Filament production

The coating continuous fibre fabrication (CCF) process was employed to make filaments with continuous fibres by extrusion coating. The influence of processing parameters such as the temperature, the extrusion rate, the line speed and the oven temperature were previously optimized in order to produce filaments with minimal defects and a low variation of diameter. A diameter of 400 µm was targeted to enhance the potential printing quality compared to current 1.75 mm thick filaments. Table 1 reports the extrusion parameters that were used continuous flax/PLA biocomposite filaments.

Table 1 Extrusion parameters to produce continuous flax/PLA filaments

	Continuous flax yarn filament
Die size (mm)	0.6 (diameter) x 20 (length)
Extruder temperature (°C)	180
Die temperature (°C)	190
Oven temperature (°C)	120
Consolidating system (mm)	40 x 7
Puller speed (m/min)	1
Extrusion speed (rpm)	5

Fibre volume content was estimated by specific gravity measurement (ASTM D792) with 5 replicates and confirmed by image analysis.

2.3 Composite production by Fused Deposition Modeling (FDM)

A Prusa i3 printer was used for the FDM, after being modified with a custom 1.8 mm nozzle. A flat-head nozzle was used to compress the filament and to drive it during printing. To control the cooling rate of the filament and to improve the printing accuracy, a second fan was fixed near the printing nozzle. An Arduino® card was used to control the fan rotation speed, allowing

it to be modified between each layer. The 3D printer was controlled by Simplify3D® software. The temperature of the nozzle and heating plate was set at 195°C and 60°C respectively, and the printing speed was 6 mm/s.

All samples were printed with a rectilinear filling pattern, oriented either 0° (longitudinal) or 90° (transverse) along the *x* axis without any contour.

2.4 Characterization of the mechanical properties

Tensile samples geometry were settled at L : 125 x W : 10 x t : 1 mm. Tensile tests were performed on longitudinally (0°) and transversely (90°) printed samples following ISO 527-4 standards, using an MTS Synergie RT1000 traction machine. A 10 kN force sensor was used to measure the load, and an axial extensometer with a nominal length of 25 mm (L_0) was used to measure the strain and then calculate the tensile modulus. The tensile modulus E_1 was determined over a range of strains between 0.05 % and 0.1 % according to the procedure suggested by Shah *et al.* [20], and a second modulus E_2 was also evaluated on a constant strain range (>0.4%). The tensile strain rate was set at 1 mm/min, and five samples were systematically tested for each determination.

2.5 Porosity content measurement

The porosity content was determined according to ASTM D2734-09 2009. The weight and volume of the composite were measured and the percentage of porosity was determined using the following equation :

$$vp = 1 - \rho_c \left(\frac{1-w_f}{\rho_m} + \frac{w_f}{\rho_f} \right) \quad (1)$$

Where v_p is the porosity content; ρ_c, ρ_m, ρ_f the composite, matrix, and fibre densities respectively; and w_f the fibre weight ratio. Results were double-checked using image analysis of composite cross sections.

2.6 Microscopic and macroscopic observations

Microscopic observations were performed with Scanning Electron Microscopy. The samples were sputter-coated with a thin layer of gold in an Edwards sputter coater and then inspected with a JEOL JSM 6460LV scanning electron microscope operated at an accelerating voltage of 20 kV. Macroscopic observations of samples were carried out with a Canon digital camera DS126441 equipped with a Sigma macro lens (70-300 mm f/4-5.6).

3. Results and Discussion

3.1 Observations on the microstructure of the filaments and the continuous flax/PLA printed biocomposites

Continuous flax/PLA biocomposites filaments (cFF/PLA) exhibit irregularities on their surface which led to non-perfectly circular filaments (Figure 1a), principally due to the co-extrusion process. This has been observed previously for continuous synthetic fibre/polymer filaments [15]. An average diameter of 482 ± 30 µm was measured here, which was slightly higher than commercial continuous glass or carbon/polyamide filaments [16], but significantly thinner than the 1.8 mm discontinuous natural fibre composite filaments that are used commonly with conventional printing devices [10][21].

As the flax yarn was initially targeted for textile applications where strength is required during weaving, a twisted architecture of fibre bundles was observed. This has a direct consequence on the porosity content and the microstructure of the filaments, resulting in an imperfect impregnation of flax yarns. Low dispersion of flax yarns within the PLA matrix was evidenced with distinct matrix and fibre-rich zones (Figure 1). Even if porosities are mostly located within the flax yarn, the porosity content v_p is encouragingly low (2.1 ± 0.6 %) when compared with filaments (as described elsewhere [21][22]) that are produced including short natural fibre

composite (8.4< v_p <47 %), or in the range of continuous glass (v_p =1.34 ± 0.13%) or carbon (v_p =1.85 ± 0.30%) reinforced polyamide filaments [15].

In addition, the flax yarn exhibited a deviation from the centre of the filament that appears to be due to the co-extrusion die. Indeed, during the co-extrusion process, the polymer flows perpendicular to the flax yarn, which results in its positioning at the edge of the filament.

Trial tests have shown that a fibre volume content above 35% within filaments led to difficulties in obtaining high-quality printed samples. Thus, in the present work the developed cFF/PLA filaments contained a lower volume fraction of 30.4 ± 0.8 % ($w_f \approx$ 34.5 %), which was close to commercial high-performance carbon/polyamide filaments [15][16]. Printing filaments did not affect fibre content and therefore cFF/PLA biocomposites had a similar fibre fraction than those of filaments.

Figure 1b shows a cross-section (Y-Z plane) of a unidirectional (UD) printed composite based on cFF/PLA filaments. Overall, the microstructure was assumed to be homogeneous at the sample scale. The reinforcement was distributed homogeneously within the section according to the printing pattern. The distance between each printed yarn centre was 621 ± 54 µm, while the average thickness of a single printed layer was 252 ± 22 µm. Compared to the initial filament dimension (mean diameter 482 ± 30 µm), it is obvious that the optimized printing parameters selected for the present work implied a compression of the melted filaments which reduced the thickness and increased their width. This resulted in an encouragingly low porosity content of 3.2 ± 0.7 %, especially when compared with the literature values for 3D printed biocomposites ($v_p \approx$ 14.7-21.8%) [21] or with continuous synthetic fibres (glass or carbon)/polyamide ($v_p \approx$ 15%) [17][16][15]. As illustrated in Figure 1a and b, porosities were mainly located within the flax fibre yarn rather than between printed layers due to sufficient compression during printing.

At the mesoscale (ply scale), the microstructure appeared rather heterogeneous, made up of fibre-rich and matrix-rich areas (Figure 1b), which is directly influenced by the microstructure of the filament induced by flax yarns.

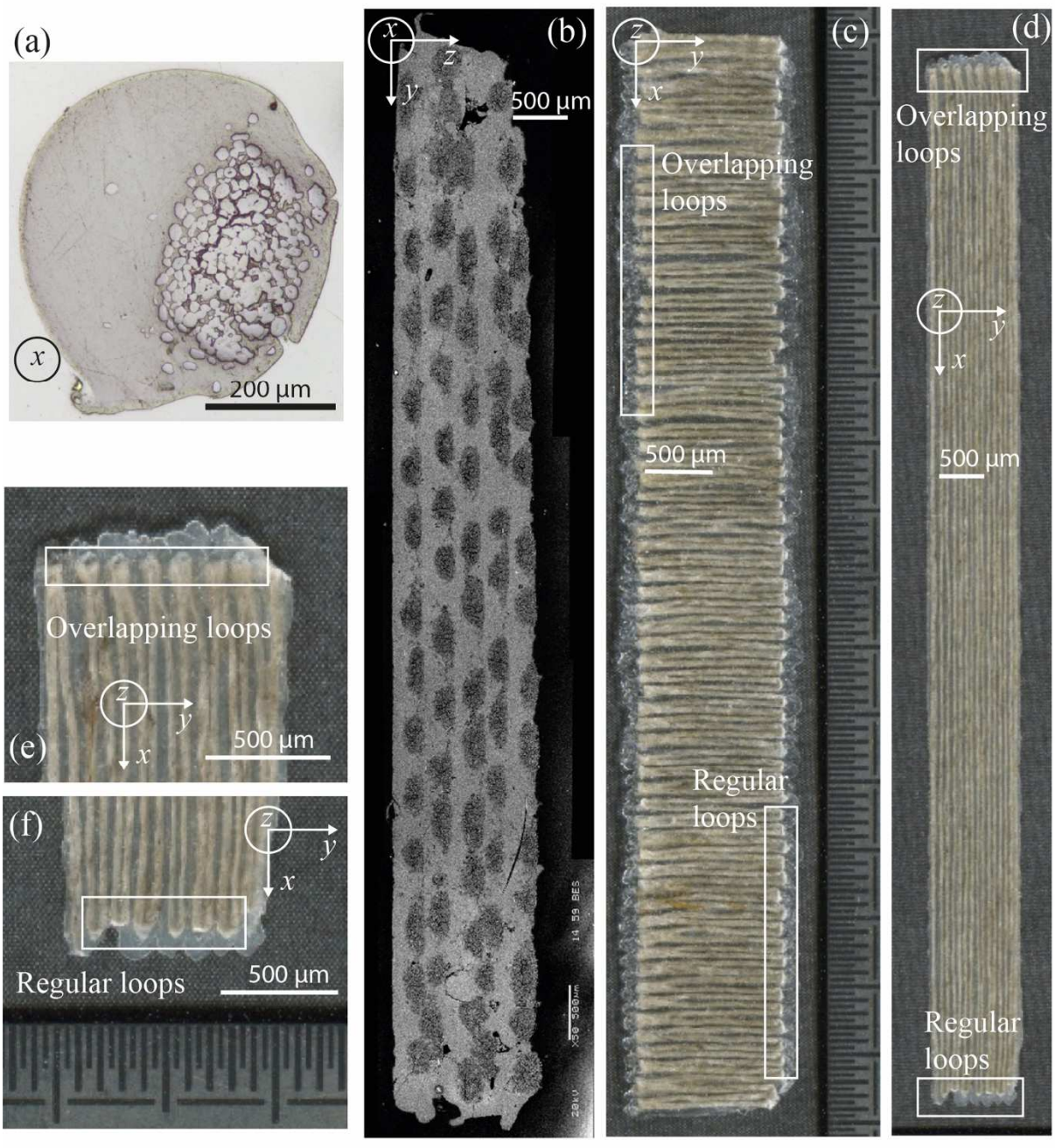

Figure 1: (a) Microstructure of a continuous flax fibre /PLA (cFF/PLA) filaments, (b) SEM microphotograph of cross section of untested cFF/PLA samples, (c) cFF/PLA transversally printed (90°) and (d) cFF/PLA longitudinally printed (0°). Details of Figure 1d showing (e) loops overlap and (f) regular loops.

Deeper analysis of the printed path was achieved by printing a single ply of continuous flax/PLA biocomposite at 0° or 90° to the *x* axis (Figure 1c and d on the X-Y plane).

Close to each sample edges (white rectangles in Figure1 e and f), the printing head achieved a turn-back that led to fibre-rich areas with potentially higher porosity content as most of porosities are located within the flax yarn (Figure 1a and b). In addition, two different patterns were observed on the opposite sample edges (white rectangles in Figure1 e and f), an overlapping of flax yarn (Figure 1e) on one side and a regular loop pattern on the other side (Figure 1f). Again, this implied local heterogeneities with a change in fibre content. As far as the authors know, this observation has not been reported in the literature on continuous fibre/Polymer composites. In the present case, it can be attributed to filament mobility inside the printing nozzle due to a geometrical mismatch ($d_{Filament} = 482.3 \pm 30$ µm and $d_{Nozzle} \approx 1000$ µm). Turning radii were measured by image analysis of the printed part without overlap. An average value of 0.29 ± 0.03 mm was obtained, which is around three times lower than the results achieved with glass and carbon fibre/PolyAmide (PA) composite using a commercial printer (Markforged® Mark two) [15]. Since the diameters of the filaments fall in the same range, the disparity in turning radius is probably due to the lower in-plane stiffness of continuous flax yarn/PLA biocomposites compared to synthetic counterparts.

3.2 Analysis of mechanical behaviour

A representative longitudinal tensile behaviour of the cFF/PLA printed biocomposite is shown in Figure 2a. Globally, tensile behaviour was similar to those reported in the literature on biocomposites manufactured by conventional manufacturing processes [20][23][24][25]. Indeed, as highlighted by the variation of tangent modulus as a function of strain, the tensile behaviour of cFF/PLA was non-linear with a large drop of stiffness after 0.4 % strain. This peculiarity is the macroscopic expression of the non-linear tensile behaviour of flax fibres at

the (sub)microscale (re-orientation of cellulose microfibrils and crystallization of amorphous cellulose [26]) when there is an efficient load transfer at the fibre/matrix interface [27]. Currently, it is difficult to define a Young's modulus that can be used for material selection or design processes. Therefore, the estimation of two elastic moduli has been proposed by Shah *et al.* [20]. The first tangent modulus (E1) was determined within a range of strain between 0.05 and 0.1% and the second modulus was the stabilized tangent stiffness (E2) determined above an applied strain of 0.4% (Figure 2a).

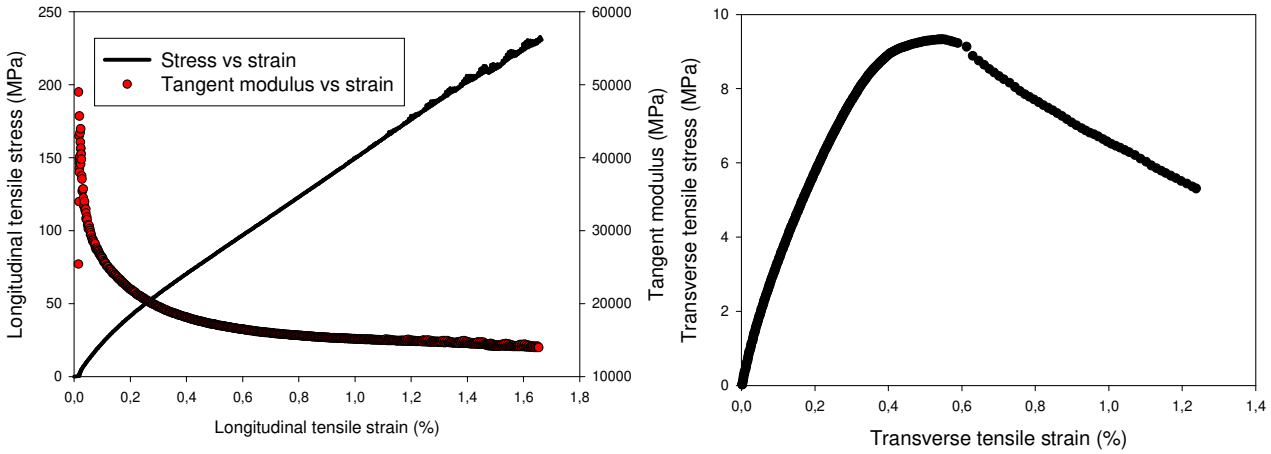

(a) (b)

Figure 2 Representative (a) longitudinal and (b) transverse tensile behaviour of a cFF/PLA biocomposite (vf =30.4%).

Fracture analysis of longitudinal cFF/PLA revealed initial transverse cracks followed by propagation along the tensile axis (Figure 3a). SEM observations highlighted that fibre breakage was associated with numerous pull-outs of flax fibres within the yarn. This demonstrates the weak yarn cohesion due to fibre bundle organization and its highly twisted structure that implies imperfect impregnation (Figure 3c). Fragile rupture of the PLA matrix was observed associated with formation of a smooth surface (white arrow on Figure 3c).

Figure 2b shows the transverse behaviour of cFF/PLA. The stress *vs.* strain curve could be divided into two parts: a first quasi-linear section was observed up to 0.4 % strain which

corresponds to fibre yarn/matrix interface debonding (Figure 3b) and flax fibre bundle debonding within the yarn. This is clearly illustrated in Figure 3c (white arrow) where a significant length of debonded flax fibres was observed. Then, a reduction of stress combined with an increasing strain revealed a quasi-ductile behaviour. Indeed, after crack initiation and propagation along fibre yarn/matrix interface (Figure 3b), an unwinding of filaments occurred (Figure 3b). This mechanism was already evidenced for continuous glass or carbon/PA parts printed composites [15] and was implied by the printing pattern with filament turn-back at sample edges.

By comparison, similar materials (Flax (30_{wf}%)/PLA) manufactured with thermocompression exhibited a brittle, *i.e.* a quasi-linear stress-strain behaviour until a sudden rupture happened around 0.8% of strain [28].

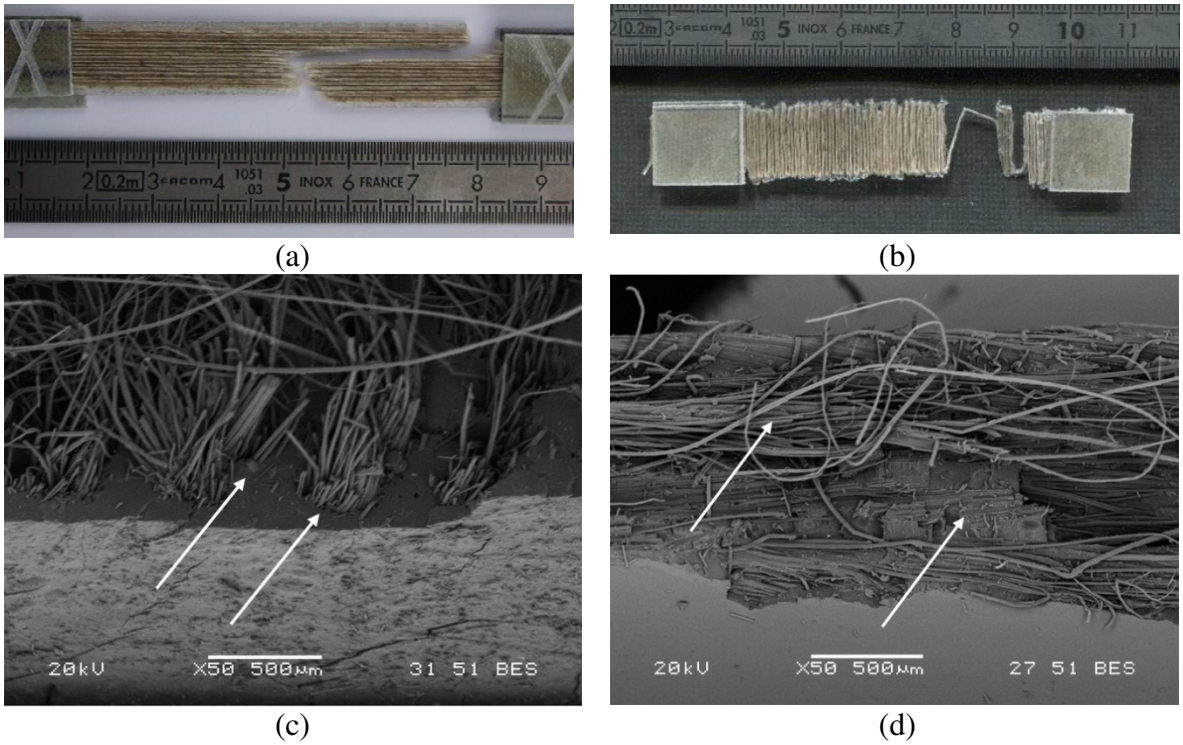

Figure 3 Macroscopic image of (a) longitudinal, (b) transverse fracture of cFF/PLA printed parts. SEM microphotograph of (c) longitudinal transverse fracture of cFF/PLA printed parts and (d) transverse fracture of cFF/PLA printed parts. White arrows evidence fibre bundle debonding and matrix failure.

3.3 Tensile mechanical properties

The tensile properties of cFF/PLA with flax fibre volume content of 30.4% ($w_f \approx 34.5\%$) were gathered in Table 2. Supplementary information (S_1) gathered results from the literature about natural fibre composites manufactured with FDM process. Overall, the longitudinal properties were significantly improved compared to those reported for pure PLA (x7 for stiffness and x4.5 for strength [29]), to discontinuous natural fibre reinforced 3D printed biocomposites (x11 for stiffness and x10 for strength) (Figure 4a), but also to the only available data on continuous jute/PLA printed biocomposites (x4.5 for stiffness and x4.5 for strength) (Figure 4a).

Table 2 Longitudinal and transverse mechanical properties of unidirectional cFF/PLA (vf = 30.4%) printed biocomposites

Material	E_{L1} (GPa)	E_{L2} (GPa)	σ_{Lmax} (MPa)	ε_{Lmax} (%)	E_T (GPa)	σ_{Tmax} (MPa)	$\varepsilon_{T\ for\ \sigma_{Tmax}}$ (%)
cFF/PLA	23.3 ± 1.8	13.6 ± 0.8	253.7 ± 15.0	1.67 ± 0.20	3.5 ± 0.45	10.8 ± 1.2	0.45 ± 0.08

This could be explained by :

- The higher mechanical properties of flax fibres [19] compared to the moderate tensile stiffness of natural fibres currently used such as wood [21], hemp [10][30], harakeke [9], coconut [31] and jute [13][32].
- The higher aspect ratio (L/d<10) of continuous flax fibre yarns compared to discontinuous fibres [9][33]. Basically, low fibre aspect ratio and length were chosen to limit the clogging effect [34] but implies an inefficient load transfer at the fibre/matrix interface, leading to debonding rather than fibre breakage.
- The higher fibre content (v_f =30.4% or w_f =34.5 %). Indeed, low fibre content between 5-20 w_f %, is generally found in the literature, which keeps viscosity relatively low and prevents clogging for discontinuous fibre biocomposites [8][9][13][21][35][36]. The use

of the simultaneous impregnation approach such as those used by Matsuzaki *et al.* [13] led also to a moderate fibre fraction. Continuous jute/PLA had a fibre volume fraction of 6.1%.

- The better homogeneity of the microstructure and lower porosity content (v_p = 3.2 ± 0.7 %) thanks to the use of a high standard textile with very low linear density of 68 Tex combined with a co-extrusion process.

Compared with 3D Printed structural composites made with continuous carbon fibres (Figure 4b), the cFF/PLA-printed biocomposites, having similar fibre volume fraction and filament production (pre-impregnated filament with co-extrusion), had logically inferior properties (stiffness and strength) considering the inferior properties of the fibres. Interestingly, they had stiffness levels similar to continuous glass fibre reinforced composites even if their strength was generally lower. Again, this is due to the difference of strength between flax and glass fibres as well as microstructure with twisted yarn and flax bundle organization. Figure 4b also evidences that continuous carbon or glass 3D printed composites could have tensile properties inferior to cFF/PLA if they were manufactured with *in-situ* impregnation. Indeed, this technique led to low fibre content and high void content. Results from the literature related to these materials were gathered in supplementary information S2.

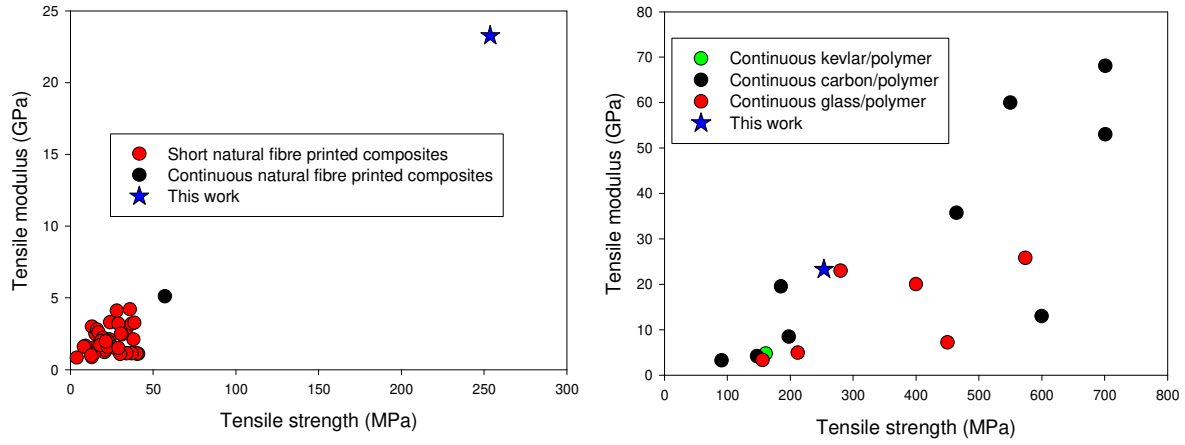

(a) (b)

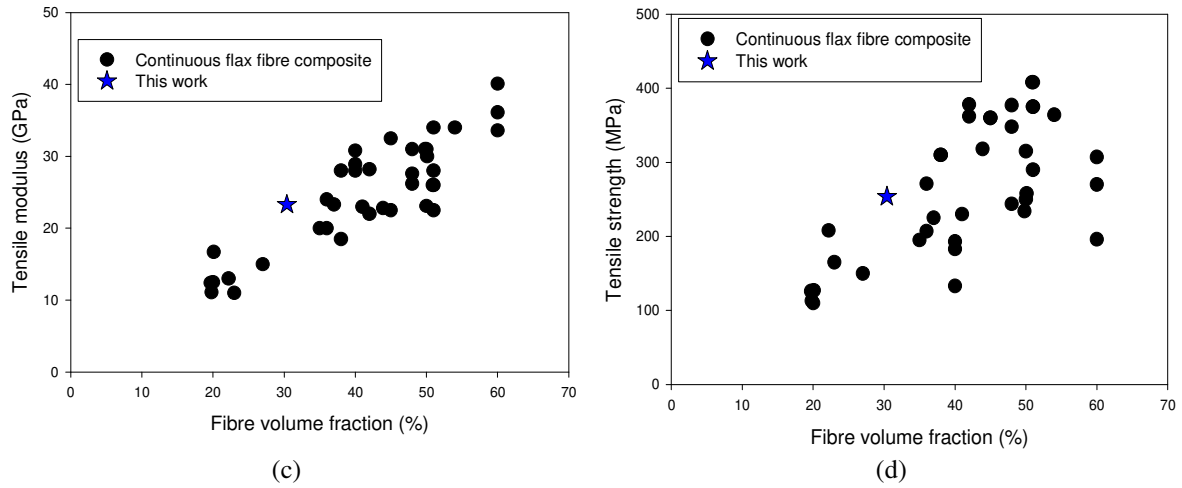

Figure 4 (a) Comparison of tensile modulus versus tensile strength for short and continuous natural fibre reinforced printed composites, [9][13][21][31][35][36][37][38][39], (b) comparison of tensile modulus versus tensile strength for continuous carbon and glass fibre printed composites [12][13][14][15][16][17][40][41][42] and comparison of (c) tensile modulus and (d) tensile strength as a function of fibre volume fraction for natural fibre composite used for structural applications manufactured with conventional process [18][25][27][43][44][45][46][47][48][49].

Then, in Figure 4c and d, the longitudinal tensile modulus (E_1) and strength of cFF/PLA were compared with continuous flax fibre composites manufactured with thermocompression or film stacking, VARTM or even Automatic Fibre Placement (AFP). The properties were plotted as a function of fibre content to ensure an appropriate comparison. This results were consistent with those of conventionally manufactured biocomposites (Figure 4c and d). Fused Deposition Modeling of continuous flax fibres/PLA could be therefore considered as a viable technique for producing high-performance biocomposites, provided that high-performance fibres were used along with high-quality coated filaments. Compared to other additive manufacturing techniques such as Automatic Fibre Placement (AFP), 3D printing of continuous flax fibre can achieve similar properties, but it is interesting to note that no additional compression step is required.

As already claimed, the tensile modulus E_1 was not sufficient to describe the behaviour of natural fibre composites, despite being the most common parameter available in the literature. cFF/PLA showed a reduction of around 40% between E_1 and E_2 which was in a range similar

to the related literature [47]. The back calculation made from the longitudinal properties of the composite, while applying a rule of mixture using E_1 or E_2, yielded a fibre stiffness E_{f1} of 68 GPa or 39 GPa, respectively. This was in agreement with the results of Baets *et al.* [49] and Bensadoun *et al.* [50]. Therefore, FDM of continuous flax fibre biocomposites enabled retaining the reinforcing potential of flax fibre even if thermal cycles were applied (co-extrusion and printing processes).

Transverse properties of cFF/PLA were also evaluated and presented in Table 2. Similar to conventional composite laminates, transverse stiffness was barely improved by the addition of natural fibres. Compared with the literature on continuous synthetic fibre 3D printed composites, the transverse stiffness of cFF/PLA was significantly higher than glass or carbon/PA composites ($E_T \approx 0{,}4$ GPa [15]) due to PLA stiffness. A similar range of transverse strength could be found. cFF/PLA composites had higher transverse stiffness and strength than Elium®/flax made with VARTM [27] or MAPP/Flax made with Automatic Fibre Placement [44], but lower than unidirectional flax/PLA manufactured by thermocompression, ($E_{T\ flax/PLA}$= 4.15 ± 0.35 MPa and $\sigma_{T\ flax/PLA}$ = 27 ± 3.3 MPa)[28].

These properties were found to be the result of :

- The printing pattern with loop formation at the edge of the sample. Indeed, during a tensile test, two non-overlapping filaments came apart, leading to unwinding and rupture (Figure. 4b).
- The heterogeneous microstructure with a fibre-rich area, due to twisted yarn but also the printing pattern's implied stress concentration.
- The twisted yarn that led to incomplete polymer impregnation and a low transverse cohesion of yarn (reduced area of fibre/fibre interface) within the composite (Figure 4d).

Finally, printing cFF/PLA enabled (us to reach/reaching) a ratio of longitudinal to transverse stiffness (anisotropic ratio, *i.e.* AR) of between 4 and 7, depending on the selection of E_1 or E_2.

This ratio was found to be significantly higher than those observed for short wood fibres / PLA biocomposites (having AR ≈ 1) [21] due to better control of the fibre orientation. Therefore, printing continuous natural fibre like cFF/PLA offered better control of mechanical performance than short fibre biocomposite counterparts. It also opened the design envelope for biocomposites through potential gradual material and even 4D printing [51].

4. CONCLUSION

This study presented a novel continuous flax fibre/PLA biocomposite (cFF/PLA) manufactured using an affordable open-access 3D printing device, which led to an important improvement compared to neat PLA, to discontinuous natural fibre printed biocomposites, and to the only available reference on continuous natural fibre printed composite (x4.5 for tensile stiffness and x4.5 for tensile strength).

To achieve this level of performance, two strategies were combined in the present work. First, unlike most of the papers in the literature on 3D printing of natural fibre biocomposites, which were focused on discontinuous fibres, the authors here have developed a filament made of a continuous natural fibre yarn coated with a PLA matrix. Second, flax fibre yarns were selected with a very low linear weight (68 Tex). Indeed, among natural fibres, flax fibres exhibit almost the best tensile properties while a low linear weight allowed a reduction in microstructural heterogeneities.

When observed at different scales, the microstructure reflected a homogeneous distribution of yarn within the cross section (macroscale). However, the twisted flax yarn used here prevented a full impregnation and led to rich-fibre areas (mesoscale).

The non-linear tensile behaviour was found to be typical of natural fibre unidirectional composites with properties that were comparable to those of long flax fibre composites

manufactured by thermocompression, VARTM, and AFP, as well as continuous glass/PA composites produced by a commercial 3D printer. Such high measured performance opens up 3D printed biocomposites to structural applications.

The weakest point of cFF/PLA printed composites was their transverse properties that remained lower than similar flax/PLA thermocompressed composites. The damage mechanism observed during tensile tests was similar to that observed in continuous synthetic fibre/polymer printed composites with filaments unwinding.

Future work should be driven to further improve the quality of the flax fibre yarn and its filaments, especially by using untwisted ribbons.

Acknowledgements

The authors wish to thank Anthony Duval from Safilin SAS for supplying the flax yarn, Yves-Marie Corre and Clément Denoual from Compositic for fruitful discussions. Michael Carpenter and Charles Ryan Hampton post-edited the English style and grammar.

REFERENCES

[1] TD. Ngo, A Kashani, G Imbalzano, KTQ. Nguyen DH. Additive manufacturing (3D printing): A review of materials, methods, applications and challenges. Compos Part B 2018.

[2] Wang X, Jiang M, Zhou Z, Gou J HD. 3D printing of polymer matrix composites: A review and prospective. Compos Part B Eng 2017;110:442–58.

[3] Faruk O, Bledzki AK, Fink H-P, Sain M. Biocomposites reinforced with natural fibers: 2000–2010. Prog Polym Sci 2012;37:1552–96. doi:10.1016/j.progpolymsci.2012.04.003.

[4] Le Duigou A, Davies P, C. B. Substitution of glass/polyester composites by Flax/PLLA biocomposites. Is is justified ? J Biobased Mater Bioenergy 2011;5:466–82.

[5] Mohanty A, Misra M, Drzal L. Sustainable Bio-Composites from Renewable Resources. J Polym Environ 2002;10:19–26.

[6] Pickering KL, Efendy MGA, Le TM. A review of recent developments in natural fibre composites and their mechanical performance. Compos Part A Appl Sci Manuf 2016;83:98–112. doi:10.1016/j.compositesa.2015.08.038.

[7] Ibrahim M, Badrishah NS, Sa'ude N, Ibrahim MHI. Sustainable Natural Bio Composite for FDM Feedstocks. Appl Mech Mater 2014;607:65–9.

doi:10.4028/www.scientific.net/AMM.607.65.
[8] M. Kariz, M. Sernek, M. Obućina, and M. K. Kuzman. Effect of wood content in FDM filament on properties of 3D printed parts. Mater Today 2017.
[9] M. Milosevic, D. Stoof, and K. L. Pickering. Characterizing the Mechanical Properties of Fused Deposition Modelling Natural Fiber Recycled Polypropylene Composites. J Compos Sci 2017;1:7.
[10] D. Stoof and K. Pickering. Fused Deposition Modelling of Natural Fibre/Polylactic Acid Composites. J Compos Sci 2017;1:8.
[11] Goh GD, Yap YL, Agarwala S, Yeong WY. Recent progress in Additive Manufacturing of Fiber Reinforced Polymer Composite. AdvMater Technol 2019;4.
[12] Li N, Li Y, Liu S. Rapid prototyping of continuous carbon fiber reinforced polylactic acid composites by 3D printing. J Mater Process Technol 2016;238:218–25. doi:10.1016/j.jmatprotec.2016.07.025.
[13] Matsuzaki R, Ueda M, Namiki M, Jeong T-K, Asahara H, Horiguchi K, et al. Three-dimensional printing of continuous-fiber composites by in-nozzle impregnation. Sci Rep 2016;6:23058. doi:10.1038/srep23058.
[14] Yang C, Wiaoyong T, Liu T, Cao Y, Li D. 3D printing for continuous fiber reinforced thermoplastic composites : mechanism and performance. Rapid Prototyp J 2017;23.
[15] Chabaud G, Castro M, Denoual C, Le Duigou A. Hygromechanical properties of 3D printed continuous carbon and glass fibre reinforced polyamide composite for outdoor structural applications. Addit Manuf 2019;26:94–105.
[16] G.D. Goh, V. Dikshit, A.P. Nagalingam, G.L. Goh, S. Agarwala, S.L. Sing, J.Wei, W.Y. Yeong. Characterization of mechanical properties and fracture mode of additively manufactured carbon fiber and glass fiber reinforced thermoplastics. Mater Des 2018;137:79–89.
[17] Dickson AN, Barry JN, McDonnell KA, Dowling DP. Fabrication of continuous carbon, glass and Kevlar fibre reinforced polymer composites using additive manufacturing. Addit Manuf 2017;16:146–52. doi:10.1016/j.addma.2017.06.004.
[18] Baley C, Lan M, Bourmaud A, Le Duigou A. Compressive and tensile behaviour of unidirectional composites reinforced by natural fibres: Influence of fibres (flax and jute), matrix and fibre volume fraction. Mater Today Commun 2018:DOI: 10.1016/j.mtcomm.2018.07.003.
[19] Baley C, Bourmaud A. Average tensile properties of French elementary flax fibers. Mater Lett 2014;122:159–61. doi:http://dx.doi.org/10.1016/j.matlet.2014.02.030.
[20] Shah DU. Damage in biocomposites: Stiffness evolution of aligned plant fibre composites during monotonic and cyclic fatigue loading. Compos Part A Appl Sci Manuf 2015. doi:10.1016/j.compositesa.2015.09.008.
[21] Le Duigou A, Castro M, Bevan R, Martin N. 3D printing of wood fibre biocomposites: From mechanical to actuation functionality. Mater Des 2016;96:106–14. doi:10.1016/j.matdes.2016.02.018.
[22] Filgueira D, S Holmen, JK. Melbø, D Moldes, AT. Echtermeyer GC-C. 3D Printable Filaments Made of Biobased Polyethylene Biocomposites. Polymers (Basel) 2018;10:314.
[23] Cherif ZE, Poilâne C, Vivet A, Ben Doudou B, Chen J. About optimal architecture of plant fibre textile composite for mechanical and sorption properties. Compos Struct 2016;140:240–51. doi:10.1016/j.compstruct.2015.12.030.
[24] Baley C, Le Duigou A, Bourmaud A, Davies P. Influence of drying on the mechanical behaviour of flax fibres and their unidirectional composites. Compos Part A Appl Sci

Manuf 2012;43:1226–33. doi:10.1016/j.compositesa.2012.03.005.
[25] Bourmaud A, Le Duigou A, Gourier C, Baley C. Influence of processing temperature on mechanical performance of unidirectional polyamide 11 - flax fibre composites. Ind Crops Prod 2016;84:151–65. doi:10.1016/j.indcrop.2016.02.007.
[26] Placet V, Cissé O, Lamine Boubakar M. Nonlinear tensile behaviour of elementary hemp fibres. Part I: Investigation of the possible origins using repeated progressive loading with in situ microscopic observations. Compos Part A Appl Sci Manuf 2014;56:319–27. doi:10.1016/j.compositesa.2012.11.019.
[27] Monti A, El Mahi A, Jendli Z, Guillaumat L. Mechanical behaviour and damage mechanisms analysis of a flax-fibre reinforced composite by acoustic emission. Compos Part A Appl Sci Manuf 2016;90:100–10. doi:10.1016/j.compositesa.2016.07.002.
[28] Le Duigou A, Baley C, Grohens Y, Davies P, Cognard J-Y, Créach'Cadec R, et al. A multi-scale study of the interface between natural fibres and a biopolymer. Compos Part A Appl Sci Manuf 2014;65. doi:10.1016/j.compositesa.2014.06.010.
[29] Letcher T, Waytahek M. Material property testing of 3D printed specimen in PLA on an entry-level 3D printer. Proc ASME 2014 Int Mech Eng Congr Expo 2014;IMECE2014-.
[30] Stoof D, Pickering K. 3D Printing of Natural Fibre Reinforced Recycled Polypropylene. Process Fabr Adv Mater 2017:668–91.
[31] Safka J, Ackermann M, Bobeck J, Seidl M, Habr J BL. Use of composite materials for FDM 3D print technology. Mater Sci Forum 2016;862:174–81.
[32] Torrado AR, Roberson DA. Failure Analysis and Anisotropy Evaluation of 3D-Printed Tensile Test Specimens of Different Geometries and Print Raster Patterns. J Fail Anal Prev 2016;16:154–64. doi:10.1007/s11668-016-0067-4.
[33] Depuydt D, Balthazar M, Hendrickx K, Six W, Ferraris E, Desplentere F, et al. Production and characterization of bamboo and flax fiber reinforced polylactic acid filaments for fused deposition modeling (FDM). Polym Compos 2018:DOI 10.1002/pc.24971.
[34] Kariz M, Sernek M, Obucina M KM. Effect of wood content in FDM filament on properties of 3D printed parts. Mater Today Commun 2018;14:135–40.
[35] Stoof D, Pickering K. Fused Deposition Modelling of Natural Fibre/Polylactic Acid Composites. J Compos Sci 2017;1:8. doi:10.3390/jcs1010008.
[36] D. Stoof and K. Pickering. Sustainable composite fused deposition modelling filament using recycled pre-consumer polypropylene. Compos Part B Eng 2018;135:110–8.
[37] Torrado Perez AR, Roberson DA, Wicker RB. Fracture surface anlysis of 3D printed tensiles specimens of novel ABS based materials. J Fail Anal Preven 2014;14:343–53.
[38] Tarrés Q, Melbø JK, Delgado-Aguilar M, Espinach FX, Mutjé P, Chinga-Carrasco G. Bio-polyethylene reinforced with thermomechanical pulp fibers: Mechanical and micromechanical characterization and its application in 3D-printing by fused deposition modelling. Compos Part B Eng 2018;153:10–7.
[39] Yang TC. Effect of extrusion temperature on the physico-mechanical properties of unidirectional wood fiber reinforced polylactic acid composite (WFRPC) components using Fused deposition modeling. Polymers (Basel) 2018;10:1–11.
[40] Van Der Klift F, Koga Y, Todoroki A, Ueda M, Hirano Y, Matsuzaki R. 3D Printing of Continuous Carbon Fibre Reinforced Thermo-Plastic (CFRTP) Tensile Test Specimens. Open J Compos Mater 2016;06:18–27. doi:10.4236/ojcm.2016.61003.
[41] Justo J, Távara∗ L, García-Guzmán L, F. París. Characterization of 3D printed

longfibre reinforced composites. Compos Struct 2018;185:537–48.
[42] Tian X, Liu T, Wang Q, Dilmurat A, Li D, G. Ziegmann. Recycling and remanufacturing of 3D printed continuous carbon fiber reinforced PLA composites. J Clean Prod 2017;142:1609–18.
[43] Coroller G, Lefeuvre A, Le Duigou A, Bourmaud A, Ausias G, Gaudry T, et al. Effect of flax fibres individualisation on tensile failure of flax/epoxy unidirectional composite. Compos Part A Appl Sci Manuf 2013;51. doi:10.1016/j.compositesa.2013.03.018.
[44] C Baley, A Kervoëlen, M Lan, D Cartié, A Le Duigou, A Bourmaud PD. Flax/PP manufacture by automated fibre placement (AFP). Mater Des 2016;94:207–13.
[45] Liang S, Gning P-B, Guillaumat L. Quasi-static behaviour and damage assessment of flax/epoxy composites. Mater Des 2015;67:344–53. doi:10.1016/j.matdes.2014.11.048.
[46] Lefeuvre A, Bourmaud A, Baley C. Optimization of the mechanical performance of UD flax/epoxy composites by selection of fibres along the stem. Compos Part A Appl Sci Manuf 2015;77:204–8. doi:10.1016/j.compositesa.2015.07.009.
[47] Cadu T, Berges M, Sicot O, Person V, Piezel B, Van Schoors L, et al. What are the key parameters to produce a high-grade bio-based composite? Application to flax/epoxy UD laminates produced by thermocompression. Compos Part B Eng 2018;150:36–46.
[48] Van de Weyenberg I, Ivens J, De Coster A, Kino B, Baetens E, Verpoest I. Influence of processing and chemical treatment of flax fibres on their composites. Compos Sci Technol 2003;63:1241–6. doi:10.1016/S0266-3538(03)00093-9.
[49] Baets J, Plastria D, Ivens J, Verpoest I. Determination of the optimal flax fibre preparation for use in unidirectional flax–epoxy composites. J Reinf Plast Compos 2014;33 :493–502. doi:10.1177/0731684413518620.
[50] Bensadoun F, Verpoest I, Baets J, Müssig J, Graupner N, Davies P, et al. Impregnated Fibre Bundle Test for Natural Fibres used in Composites. J Reinf Plast Compos 2017;36:942–57. doi:10.1177/0731684417695461.
[51] A Le Duigou, S Requile, F Scarpa, M Castro, A Le Duigou, S Requile, F Scarpa, M Castro. Natural fibres actuators for smart bio-inspired hygromorph biocomposites. Smart Mater Struct 2017:125009.
[52] Yang T. Effect of Extrusion Temperature on the Physico-Mechanical Properties of UnidirectionalWood Fiber-Reinforced Polylactic Acid Composite (WFRPC) Components Using Fused DepositionModeling. Polymers (Basel) 2018;10:doi:10.3390/polym10090976.
[53] Roberston DA, Rocha CR PM. Evaluation of 3D printable sustainable composites. http://sffsymposium.engr.utexas.edu/sites/default/files/2015/2015-75-Roberson.pdf 205AD.

Supplementary information

S.1 Tensile properties of natural fibre printed biocomposites

Materials	M_f (%)	Tensile modulus (GPa)	Tensile strength (MPa)	Ref.
Hemp/rPP	10	2.5	15	[9]
	20	3	13	
	30	2.8	16	
Harakeke/rPP	10	2.6	17	
	20	3.3	24	
	30	2.1	22	
Wood/PLA/PHA	15.2	2.2±0.1	19.6±1.5	[21]
		2.0±0.05	18.5±0.7	
		1.55±0.1	14.4±0.5	
		1.65±0.06	9.1±0.4	
		1.6±0.2	8±2	
		0.8±0.1	3.9±0.7	
Harekeke/PLA	10	2.9	34	[10]
	20	4.2	37	
	30	4.1	28	
Hemp/PLA	10	3.2	37	
	20	3.2	29	
	30	x	24	
Harekeke/rPP	10	1.4	19.9	[36]
	20	1.85	22.1	
	30	2.1	23.6	
Hemp/rPP	10	1.2	20.5	
	20	1.4	21	
	30	2.0	22.45	
Jute/ABS	5	1.5±0.1	25.9	[37]
		0.9±0.2	12.9	
Wood/PLA	20	1.1	14	
Wood/PLA	40	1.8±0.03	20±0.5	[52]
		1.7±0.06	19.5±1.0	
		1.7±0.01	18±0.1	
		1.7±0.04	18.1±0.4	
Cellulose pulp/PE	10	0.98±0.07	12.5	[38]
	20	1.51±0.12	29	
Coir/ABS	15	1.95	21.4	[31]
Jute/PLA	5	2.1	38	[53]
Continuous jute/PLA	6.1	5.1±0.4	57.1±5.3	[13]

S.2 Tensile properties of continuous synthetic fibre printed composites

Materials	M_f (%)	Tensile modulus (GPa)	Tensile strength (MPa)	Ref.
Carbon/PLA	9	19.5±2.1	185.2±24.6	[13]
Carbon/PLA	42	3.25	91	[12]
Carbon/PLA		0.72	80	
Carbon/ABS	10	4.2	147	[14]
Carbon/PA	18.2	26.7±4.8	298.1±47	[15]
	31	41.1±3.1	442.9±38	
	39	52.0±4.4	x	
	44.5	60.1±7.0	533±41	
Carbon/PA	49.6	69.1±6.0	700±70	[41]
Carbon/PA	50.7	13±1	600±30	[16]
Carbon/PA	44	35.7	464	[40]
Carbon/PLA	13	20.6	256	[42]
Glass/PA	37.5	16.4±5.0	329.8±80	[15]
	46	19.3±2.8	381.1±26.4	
	52	24.2±2.6	x	
	58.4	28.9±2.3	264±53	
Glass/PA	16	3.12±0.15	194±1	[17]
	19.6	3.75±0.89	206±5	
Glass/PA	68.5	25.9±1.9	574.6±35.7	[41]
Glass/PA	54	7.2±0.01	450±1	[16]
Kevlar/PA	11.5	3.61±0.54	150±10	[17]
	14.5	4.37±0.59	164±9	